RSC Advances

PAPER

View Article Online
View Journal | View Issue

Check for updates

Cite this: *RSC Adv.*, 2018, **8**, 14925

# Nontargeted SWATH acquisition mode for metabolites identification of osthole in rats using ultra-high-performance liquid chromatography coupled to quadrupole time-of-flight mass spectrometry†

Man Liao, Xinpeng Diao, Xiaoye Cheng, Yupeng Sun and Lantong Zhang *

Osthole (OST), 7-methoxy-8-isopentenoxycoumarin, is the characteristic constituent found in *Cnidium monnieri* (L.) Cuss. and possesses excellent pharmacological activities, including anticancer, anti-apoptosis and neuroprotection. In this study, a rapid and reliable method based on ultra-high-performance liquid chromatography coupled to quadrupole time-of-flight mass spectrometry (UHPLC-Q-TOF-MS) and MetabolitePilot2.0™ software with principal component variable grouping (PCVG) filtering was developed to observe probable metabolites of OST firstly. The high resolution mass data were acquired by data-independent acquisition mode (DIA), *i.e.*, sequential window acquisition of all theoretical fragmentation spectra (SWATH), which could significantly improved the hit rate of low-level and trace metabolites. A novel data processing method 'key product ions (KPIs)' were employed for metabolites rapid hunting and identification as an assistant tool. A total of 72 metabolites of OST were detected *in vitro* and *in vivo*, including 39 metabolites in rat liver microsomes (RLMs), 20 metabolites in plasma, 32 metabolites in bile, 32 metabolites in urine and 37 metabolites in feces. The results showed that mono-oxidation, demethylation, dehydrogenation, sulfate conjugation and glucuronide conjugation were major metabolic reactions of OST. More significant, oxydrolysis, 3,4-epoxide-aldehylation, phosphorylation, *S*-cysteine conjugation and *N*-acetylcysteine conjugation were considered as unique metabolic pathways of OST, and phosphorylation, *S*-cysteine conjugation and *N*-acetylcysteine conjugation reactions were characterized in rat biological samples for the first time. Preparation of active metabolites will be greatly helpful in elucidating the potential biological mechanism of OST, and the proposed metabolic pathways of it might provide further understanding of the safety and efficacy of simple coumarins.

Received 8th February 2018
Accepted 23rd March 2018

DOI: 10.1039/c8ra01221k

rsc.li/rsc-advances

Open Access Article. Published on 19 April 2018. Downloaded on 3/9/2025 2:44:59 PM.
This article is licensed under a Creative Commons Attribution-NonCommercial 3.0 Unported Licence.

## 1. Introduction

Osthole (OST, Fig. 1), a natural simple coumarin, is the active component in many popular medical plants and fruits, including *Cnidium monnieri* (L.) Cuss.[1] *Peucedanum ostruthium*,[2] *Citrus aurantium*[3] and *C. sinensis* cv. Doppio Sanguigno.[4] In recent years, pharmacological studies have revealed that OST had diverse effects as anticancer,[5] anti-apoptosis[6,7] and neuroprotection.[8,9] Currently, OST has attracted tremendous attention due to its insect control application on crop planting and it has become a novel plant-based pesticides at home and abroad.[3,10,11]

Prototype drugs undergoes rapid metabolism after administration and the metabolites might exert higher biological activity or reduce the toxicity.[12] Tsai T. H. *et al.*,[13] Liu M. *et al.*[14] and Yun F. *et al.*[15] all developed the determination of OST in rat plasma and indicated that OST appeared to be absorbed fast but eliminated slowly. So, it is vital to investigate biotransformation of OST *in vitro* and *in vivo* to ensure further safety and efficacy.

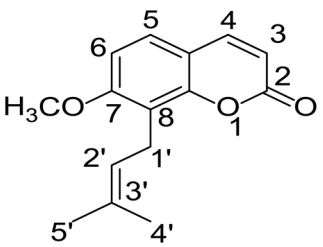


Fig. 1 Chemical structure of osthole.

*Department of Pharmaceutical Analysis, School of Pharmacy, Hebei Medical University, 361 East Zhongshan Road, Shijiazhuang, Hebei 050017, P. R. China. E-mail: zhanglantong@263.net; Fax: +86-311-86266419; Tel: +86-311-86266419*

† Electronic supplementary information (ESI) available. See DOI: 10.1039/c8ra01221k

Open Access Article. Published on 19 April 2018. Downloaded on 3/9/2025 2:44:59 PM.
This article is licensed under a Creative Commons Attribution-NonCommercial 3.0 Unported Licence.

To our knowledge, only eighteen metabolites of OST were tentatively identified in rat urine by UPLC-QTOF/MS involving 7-demethylation, 8-dehydrogenation, hydroxylation, 3,4-epoxide, glucuronide conjugation and sulfate conjugation metabolic pathways.[16,17] Lv X. *et al.*[18] observed thirteen metabolites in rat urine after oral administration of OST by HPLC-DAD-MS/MS analysis and 2D-NMR techniques. Besides, five demethylation or multiple isomers of dehydrogenation metabolites were observed in rat liver microsomes using HPLC-Qtrap-MS/MS.[19] Liver is considered as the most important organ in the biotransformation of drugs with a variety of required enzymes especially for cytochrome P450 (CYP450) enzymes.[20] Zhang L. F. *et al.*[21] investigated that OST presented characteristics of enzymatic kinetics metabolism in rat hepatocytes and CYP3A4 was involved in the metabolism of OST *in vitro*. Xiao H. *et al.*[22] showed that ketoconazole, sulfaphenazole and quinidine could inhibit the disappearance of OST and CYP3A4 was involved in the metabolism of OST at all the tested concentrations of OST. However, CYP2C9 and CYP2D6 mediated the metabolism at high concentration of OST.

As a predominant analytical technique for unknown compounds analysis, high-resolution mass spectrometry (HRMS) especially TOF analyzer[23] plays an important role in qualitative studies of metabolites with higher accuracy and sensitivity. 'Data-independent acquisition' (DIA) strategies, *i.e.*, sequential window acquisition of all theoretical fragment spectra (SWATH), have been developed in the study of metabolite identification[24,25] and proteomics[26] recently, which could acquire whole precursor ions at any time in the chromatographic separation by parsing the mass range into small specific mass windows. In every scan cycle, the analyzer rapidly and sequentially acquires high hit rates of MS/MS spectra of all mass windows across the specific mass range.[24] A practical analysis strategy, which combined Principal Component Variable Grouping (PCVG) filtering in the MetabolitePilot™2.0 software and key product ions (KPIs) in Masterview™1.1 post-processing software, holds the advantage of eliminating hybrid spectra and rapidly hunting possible metabolites. The assistant data processing techniques possessed in MetabolitePilot™2.0 software, including extracted ion chromatography (EIC), mass defect filtering (MDF), production filtering (PIF), neutral loss filtering (NLF) and isotope pattern filtering (IPF) could also be used to analyze the structures of metabolites.[25] Therefore, it is essential to explore metabolism of OST *in vitro* in the hepatic model and *in vivo* metabolism in rats by a powerful and novel analytical technique for metabolite identification in complex matrices with its high resolution and accurate mass measurements.

# 2. Material and methods

## 2.1. Chemicals and reagents

OST (purity > 98%, 110822-200305) which was extracted from *Cnidii fructus* was applied by National Institutes for Food and Drug Control. Isoscopoletin (purity > 98%, 111741-200501) was also purchased from National Institutes for Food and Drug Control. Daphnetin (purity > 98%, MUST-13071104) was purchased from Chengdu Mansite Bio-Technology Co., Ltd. Isopsoralen (purity > 98%, YJ-131203) and 7-hydroxycoumarin (purity > 98%, J0222AS) were purchased from Jiangsu Yongjian Pharmaceutical Co., Ltd. and Dalian Meilun Biotech Co., Ltd., respectively. RLMs were laboratory-made[27] and the protein concentration of them was determined by the Lowry method in Department of Pharmaceutical Analysis in School of Pharmacy of Hebei Medical University. They were stored at −80 °C until being used. Phosphate buffer saline (PBS, 10×), β-nicotinamide adenine dinucleotide phosphate (NADPH, purity > 98%) in reduced form, UDP-D-glucuronide trisodium salt (UDPGA, purity > 98%) and alamethicin (purity > 98%) were purchased from Solarbio Science Co., Ltd. (Beijing, China). Magnesium chloride hexa-hydrate was obtained from Yong Da Chemical Co., Ltd. (Tianjin, China). Sodium carboxymethyl cellulose (CMC-Na) was purchased from Tianjin Chemical Co., Ltd. (Tianjin, China). These chemicals were all of analytical grade. Acetonitrile, methanol and formic acid were HPLC grade, which were purchased from Fisher Scientific (Waltham, MA, USA). De-ionized water (18.2 MΩ $cm^{-1}$) was prepared by Milli-Q water purification system (Millipore, Bedford, MA, USA).

## 2.2. Standard solutions preparation

OST was dissolved in 90% methanol at the exact concentrations of 1.13 mg $mL^{-1}$ prepared for *in vitro* incubation in RLMs. Isoscopoletin, daphnetin, 7-hydroxycoumarin and isopsoralen were weighed appropriately and dissolved in 90% methanol to reach their limit of detections.

## 2.3. Apparatus

UHPLC was performed on a Nexera-X2 UHPLC system (Shimadzu Corp., Kyoto, Japan), which consisted of two LC-30AD pumps, a SIL-30AC autosampler, a CTO-30A column oven, a CBM-20A system controller and a DGU-20A on-line degassing unit. Chromatographic separations were achieved on a Poroshell 120 EC-$C_{18}$ column (100 mm × 2.1 mm, i.d. 2.6 μm) with a Poroshell 120 EC-$C_{18}$ UHPLC guard column (Agilent Corp, Santa Clara, CA, USA). Mass spectrometry detection was performed on a hybrid quadrupole time-of-flight tandem mass spectrometer equipped with Turbo V sources and a Turbo ion spray interface (AB Sciex Triple-TOF 5600+, Concord, Ontario, Canada).

## 2.4. UHPLC-Q-TOF-MS conditions

The mobile phases consisted of eluent A (0.1% formic acid in water, v/v) and eluent B (acetonitrile). The gradient elution program was described as follows: 0–2 min, 20% B; 2–25 min, 20–60% B, 25–26 min, 60–95% B, 26–30 min, 95% B. Before the next injection, the program would maintain for 3 min for the column equilibration. The injection volume was 3 μL and the flow rate was 0.3 mL $min^{-1}$. The column was maintained at 25 °C and the autosampler tray temperature was set at 4 °C.

The optimized parameters of MS analysis were set as follows: nebulizing gas (GAS1): 55 psi, TIS gas (GAS2): 55 psi, turbo spray temperature: 550 °C and ion spray voltage (IS): 5500 V with 35 psi curtain gas. Intact protonated molecular ions $[M + H]^+$ were detected *via* TOF MS scan (60 V declustering potential (DP)),

 This journal is © The Royal Society of Chemistry 2018

Open Access Article. Published on 19 April 2018. Downloaded on 3/9/2025 2:44:59 PM.
This article is licensed under a Creative Commons Attribution-NonCommercial 3.0 Unported Licence.

30 eV collision energy (CE), 100–800 Da TOF MS scan range, and 50 ms accumulation time. SWATH MS/MS experiments acquired spectra in high sensitivity mode (60 V DP, 35 eV CE with ±15 eV collision energy spread, 50–600 Da TOF MS scan range, and 160 ms accumulation time). Twelve SWATH quadrupole isolation windows were 35 Da wide ranging from 100 to 500 Da. The total cycle time for the TOF MS and twelve SWATH MS/MS scans was 2000 ms.

### 2.5. *In vitro* metabolism of OST by RLMs

**2.5.1. Phase I metabolism.** A typical incubation mixture[27] was developed in a 0.1 mol $L^{-1}$ phosphate buffer (pH 7.4) containing 23.1 μmol $L^{-1}$ OST, 0.4 mg rat liver microsomal protein from male Sprague Dawley rats, 3.3 mmol $L^{-1}$ $MgCl_2$ and 2.0 mmol $L^{-1}$ β-NADPH in the final volume 200 μL. It must be sure that the organic solvent did not exceed 1% (v/v) in the incubation. The mixture was prewarmed for 5 min at 37 °C and initiated by adding NADPH generating system. After incubation at 37 °C for 30 min, 1.0 mL ice-cold ethyl acetate were added to stop the reaction. The mixture was extracted by vortex-mixing for 3 min and then centrifuged at 15 000 rpm at 4 °C for 10 min. The organic phase was collected and evaporated under nitrogen gas. The residues were reconstituted in 90% acetonitrile (200 μL) and the supernatant was filtered through a 0.22 μm polytetrafluoroethylene (PTFE) membrane filter and stored at −20 °C until analyzed. The control sample was incubated without NADPH generating system followed by the same treatment while the blank sample was incubated without parent drug.

**2.5.2. Phase II metabolism.** The incubation mixture contained 23.1 μmol $L^{-1}$ OST, 0.4 mg rat liver microsomal protein from male Sprague Dawley rats, 3.3 mmol $L^{-1}$ $MgCl_2$, 2.0 mmol $L^{-1}$ UDPGA and 25.0 μg $mL^{-1}$ alamethicin in 50.0 mmol $L^{-1}$ Tris–HCl buffer (pH 7.4) with a final volume of 200 μL. The organic solvent did not exceed 1% (v/v) in the incubation. The mixture was preincubated for 15 min at 37 °C and initiated by the addition of UDPGA. Reaction termination was achieved after 60 min at 37 °C by adding 0.2 mL ice-cold acetonitrile. After centrifugation at 15 000 rpm at 4 °C for 10 min, the supernatant was filtered through a 0.22 μm PTFE membrane filter and stored at −20 °C until analyzed. The control sample was incubated without UDPGA followed the same treatment while the blank sample was incubated without OST.

### 2.6. Animal and drug administration

Male Sprague Dawley rats (Certificate no. SCXK 2013-1-003, 12–14 weeks of age), weighing 240 ± 20 g, were applied by Experimental Animal Research Center, Hebei Medical University, China. The rats were maintained at ambient temperature (22–24 °C) and 60% relative humidity with a 12 h light/dark cycle. All animals were kept in an environmentally controlled breeding room for at least 1 week with water and standard chow *ad libitum*, and fasted for 12 h with free access to water before the formal tests. Then the rats were randomly divided into six groups, including three treated groups (group 2, 4 & 6) for plasma, bile, urine and feces drug samples ($n = 6$) and three control groups (group 1, 3 & 5) for blank samples ($n = 3$), respectively. Each group was maintained in metabolic cages for collection of samples separately. The suspension of OST powder was suspended in 0.4% CMC-Na water solution, and was given to rats at a dose of 40 mg $kg^{-1}$ by oral gavage. The same dose of 0.4% CMC-Na water solution was administered to rats of the control groups. All protocols in our laboratory were approved by the Guide for the Care and Use of Laboratory Animals (National Institutes of Health), and also approved by the Animal Ethics Committee of Hebei Medical University.

### 2.7. Sample collection and preparation

**2.7.1. Sample collection.** Each group was housed individually in metabolic cages for the collection of samples.

Blood sample was collected from posterior orbital venous of group 2 in heparinized tubes before (0 h) and at 0.17, 0.5, 1, 2, 3, 6, 8, 10, 12 h after administration.[13–15] Then, the samples were centrifuged at 4500 rpm for 5 min to obtain the plasma. The plasma samples from different time points were combined into one sample.

Six rats of group 4 were immediately anesthetized with urethane (1.0 g $kg^{-1}$, ip) by intraperitoneal injection and fixed on a wooden plate after administered OST by oral gavage. An abdominal incision was made and the bile duct was cannulated with PE-10 tubing (ID = 0.07 cm) for continuous collection of bile samples from 0–24 h.

Urine and feces samples were collected 48 h from group 6 after oral administration and free accessing to purified water. The urine and feces samples were combined as one sample, respectively. The blank group was administered purified water with the same treatment as the administration group. All samples were stored at −80 °C until further treatment.

**2.7.2. Sample preparations.** Three milliliters of plasma and 0.5 g feces were treated with 5-fold acetonitrile to precipitate proteins, and vortexed for 10 min twice. 3.0 mL of bile and 3.0 mL of urine were vortexed for 10 min with 3-fold ethyl acetate for three times, and combined all supernatant. Then the mixtures were centrifuged at 15 000 rpm at 4 °C for 10 min. The organic phase was removed under nitrogen gas. The blank biological samples were treated as the other samples. All samples were stored at −80 °C. Before analysis, the residues were dissolved in 90% acetonitrile (600 μL) completely and the supernatant was filtered through a 0.22 μm PTFE membrane filter.

### 2.8. Data processing

The analytic strategies were described in detail as follows: (1) the total ion current chromatograms (TIC) of samples and chemical structure of parent drug were imported into MetabolitePilot™2.0 software. (2) Primary metabolite identification was conducted by MetabolitePilot™2.0 software based on accurate measurements of *m*/*z* values and processing of the post-data obtained from PCVG, EIC, MDF, PIF, NLF and IPF screening of possible metabolites. The elemental compositions and chemical formulae of them could be calculated. Potential metabolites of target groups can be observed according to

Open Access Article. Published on 19 April 2018. Downloaded on 3/9/2025 2:44:59 PM. This article is licensed under a Creative Commons Attribution-NonCommercial 3.0 Unported Licence.

fragmentation rules of parent drug, polarity, retention times and the predicted metabolic pathways entered in the software. (3) Then, proposed metabolites inferred by current metabolic pathways could be validated after MS/MS spectra analysis or authentic standards comparison. Then the repeatable constituents in blank samples and test samples were removed by PeakView™ 2.2 software and MasterView™ 1.1 software. The mass error of quasi-molecular was limited in ±5 ppm, and the MS/MS error of the product ions was less than 20 ppm. Product ions *m/z* 189.0554 and *m/z* 91.0567 were set as the KPIs. KPIs technique, which was an assistant tool in MasterView™ 1.1 software could also observe probable isomers metabolites or metabolites with similar structures extracted by the same product ions rapidly. (4) Finally, the Clog *P* values and the minimize energy values provided by the program ChemBioDraw Ultra 14.0 were used for distinguishing isomers and accounting for the stability of the molecule, respectively.

# 3. Results and discussion

## 3.1. Fragmentation studies of OST

The chemical structure was shown in Fig. 1. The MS/MS fragmentation behavior of OST was investigated in positive ion mode (collision energy, 35 ± 15 eV) (Fig. S1†). After microsomal incubation *in vitro* and intragastric gavage (i.g.) administration to rats, OST was eluted at 19.68 min and yielded $[M + H]^+$ at *m/z* 245.1175 (1.2 ppm, elemental composition $C_{15}H_{16}O_3$) in RLMs, plasma, bile, urine and feces samples under the present chromatographic and mass spectrometry. OST gave abundant product ions at *m/z* 230.0937 and *m/z* 202.0625 *via* side-chain cleavage of the consecutive loss of $CH_2$. The major MS/MS characteristic product ions was at *m/z* 189.0554 conducted by the loss of the side-chain $C_4H_7$. Then a series of characteristic ions produced by *m/z* 189.0554 were showed at *m/z* 161.0625 $[M + H–C_4H_7–CO]^+$, *m/z* 159.0441 $[M + H–C_4H_7–CH_2O]^+$, *m/z* 131.0498 $[M + H–C_4H_7–CO–CH_2O]^+$, *m/z* 103.0554 $[M + H–C_4H_7–2CO–CH_2O]^+$, *m/z* 91.0567 $[M + H–C_5H_9–2CO–CH_2O]^+$, *m/z* 77.0404 $[M + H–C_7H_{11}–2CO–CH_2O]^+$ and *m/z* 65.0453 $[C_5H_5]^+$. The proposed fragmentation pathways of OST were exhibited in Fig. S1.†

## 3.2. Phase I metabolites identification

A total of 62 phase I metabolites were identified including 39 metabolites in RLMs, 12 metabolites in plasma, 22 metabolites in bile, 22 metabolites in urine and 36 metabolites in feces samples. M6, M30, M34 and M66 were confirmed in comparison with authentic standards daphnetin, 7-hydroxycoumarin, isopsoralen and isoscopoletin, respectively. Among them, most were produced *via* mono-oxidation, demethylation and dehydrogenation. Oxydrolysis, demethylation, 3,4-epoxide and aldehydation could be considered as the characteristic metabolic pathways of OST. Other metabolic pathways, such as loss of side-chain alkyl, loss of CO, di-oxidation, tri-oxidation, qur-oxidation, hydrolysis and hydrogenation, were also observed in the samples. Characteristic biotransformation pathways and the most abundant phase I metabolites were summarized as follows. The detail information about retention times and product ions of the other metabolites were listed in Table 1.

**3.2.1. Mono-oxidation metabolites.** Metabolites M33 ($t_R$ = 9.93 min), M49 ($t_R$ = 11.81 min), M56 ($t_R$ = 12.79 min), M63 ($t_R$ = 14.50 min), M68 ($t_R$ = 16.81 min), and M71 ($t_R$ = 18.88 min) exhibited the same molecular ion $[M + H]^+$ at *m/z* 261.1118 ($C_{15}H_{16}O_4$), which were 16 Da higher than that of OST. M33 and M49 both produced the characteristic product ions at *m/z* 243.1027 and *m/z* 189.0558, indicating that mono-oxidation might occur at the side-chain alkyl. Other product ions at *m/z* 131.0556 and *m/z* 91.0564 were all the same with that of parent drug. So M33 and M49 were tentatively measured as mono-oxidation metabolites at C-1′, C-2′, C-3′, C-4′or C-5′ of OST. M56, M63, M68 and M71 were all detected the product ion at *m/z* 205.0500 which suggested that mono-oxidation occurred at C-3, C-4, C-5 or C-6 of OST. After comparing the values of Clog *P* among them, M56, M63, M68 and M71 were tentatively identified as 6-hydroxylosthole, 5-hydroxylosthole, 3-hydroxylosthole and 4-hydroxylosthole, respectively.[17,28]

**3.2.2. Di-oxidation and tri-oxidation metabolites.** M38 ($t_R$ = 10.41 min) and M40 ($t_R$ = 10.68 min) showed the same molecular formula of $C_{15}H_{16}O_5$ ($[M + H]^+$ *m/z* 277.1071), which were 32 Da higher than that of OST, suggesting the di-oxidation metabolism of M0. Product ion at *m/z* 189.0544 produced by M38 indicated that di-oxidation might both occur at side-chain of OST.[28] However, the exact sites could not be confirmed. The characteristic product ion at *m/z* 205.0499 implied that one oxidation site of M40 was assigned on the site of C-3, C-4, C-5 or C-6, and the second oxidation site was uncertain.

**3.2.3. Dehydrogenation metabolites.** M29 ($t_R$ = 9.34 min), M36 ($t_R$ = 10.26 min) and M51 ($t_R$ = 11.83 min), all hold the protonated ion at *m/z* 243.1016, indicating that they were isomers with the molecular formula $C_{15}H_{14}O_3$, which were 2 Da (2H) lower than that of OST. Product ions at *m/z* 213.0913, *m/z* 201.0904, *m/z* 189.0556, *m/z* 159.0437 and *m/z* 131.0503 were all the characteristic ions of them. So, M29, M36 and M51 were tentatively identified as dehydrogenation metabolites at side chain.[16]

**3.2.4. Demethylation metabolites.** M57 ($t_R$ = 12.94 min) and M60 ($t_R$ = 13.60 min) showed the same molecular formula of $C_{14}H_{14}O_3$ ($[M + H]^+$ *m/z* 231.1016), which were 14 Da lower than that of OST. In the MS/MS spectrum, product ion at *m/z* 175.0396 of M60 could be inferred as loss a group of methyl at major ring C-7′s methoxy group. M57 conducted with product ion at *m/z* 189.0550 was investigated that demethylation reaction occurred at side chain.[28]

**3.2.5. Hydrolysis metabolites.** M50 ($t_R$ = 11.83 min) exhibited the molecular formula of $C_{15}H_{18}O_4$ ($[M + H]^+$ *m/z* 263.1265), 18 Da ($H_2O$) higher than that of OST. In its MS/MS spectrum, product ions at *m/z* 245.1179 $[M + H–H_2O]^+$ and *m/z* 189.0562 $[M + H–H_2O–C_4H_7]^+$ suggested that hydrolysis was most possible to occur at the ester bond.[28]

**3.2.6. Oxydrolysis metabolites.** M41 and M48 were eluted at 10.70 min and 11.51 min, respectively. They all showed the protonated ion at *m/z* 279.1219 ($C_{15}H_{18}O_5$), which was 34 Da ($H_2O_2$) higher than M0. In the MS/MS spectra of M41 and M48, the characteristic product ion at *m/z* 245.1169 could be yielded

 This journal is © The Royal Society of Chemistry 2018

Open Access Article. Published on 19 April 2018. Downloaded on 3/9/2025 2:44:59 PM.
This article is licensed under a Creative Commons Attribution-NonCommercial 3.0 Unported Licence.



Table 1 UHPLC-Q-TOF-MS/MS retention times and product ions of the metabolites of osthole *in vitro* and *in vivo*[a]

| Compound ID | Retention time (min) | Formula | Calculated *m/z* [M + H] | Experimental *m/z* [M + H] | Error (ppm) | Product ions | Potential pathways | Source | | | | |
|---|---|---|---|---|---|---|---|---|---|---|---|---|
| | | | | | | | | RLMs | P | B | U | F |
| M0 | 19.68 | $C_{15}H_{16}O_3$ | 245.1172 | 245.1175 | 1.2 | 230.0937, 202.0625, 189.0554, 161.0625, 159.0441, 131.0498, 103.0554, 91.0567 | — | + | + | + | + | + |
| M1 | 2.19 | $C_{14}H_{12}O_6S$ | 309.0427 | 309.0422 | −1.6 | 229.0860, 175.0398, 131.0494, 91.0559 | Demethylation, dehydrogenation, sulfate conjugation | | + | + | + | |
| M2 | 2.80 | $C_{15}H_{14}O_4$ | 259.0965 | 259.0960 | −1.9 | 243.1018, 189.0547, 131.0490 | Dehydrogenation, mono-oxidation | + | | | | |
| M3 | 3.51 | $C_{14}H_{12}O_4$ | 245.0808 | 245.0820 | 4.9 | 191.0325, 107.0493 | Dehydrogenation, mono-oxidation, demethylation | + | | | | + |
| M4 | 3.60 | $C_{15}H_{14}O_4$ | 259.0965 | 259.0962 | −1.2 | 243.1014, 189.0550 | Dehydrogenation, mono-oxidation | + | + | | | |
| M5 | 3.71 | $C_{12}H_{10}O_4$ | 219.0652 | 219.0654 | 0.9 | 175.0388, 147.0444 | Demethylation, loss of $C_2H_4$, mono-oxidation | + | + | + | | + |
| M6* | 4.65 | $C_9H_6O_4$ | 179.0339 | 179.0335 | −2.2 | 151.0387, 77.0402 | Demethylation, mono-oxidation, loss of $C_5H_8$ | | | | | + |
| M7 | 4.84 | $C_{15}H_{14}O_4$ | 259.0965 | 259.0962 | −1.2 | 243.1014, 189.0539 | Dehydrogenation, mono-oxidation | + | + | | | + |
| M8 | 5.18 | $C_{14}H_{14}O_4$ | 247.0965 | 247.0959 | −2.4 | 175.0393, 131.0495, 91.0560 | Demethylation, mono-oxidation | + | | | | + |
| M9 | 5.21 | $C_{14}H_{12}O_3$ | 229.0859 | 229.0856 | −1.3 | 175.0387, 103.0552, 91.0564 | Demethylation, dehydrogenation | + | | | + | + |
| M10 | 5.30 | $C_{11}H_8O_4$ | 205.0495 | 205.0501 | 2.9 | 175.0381, 131.0499, 91.0560 | Demethylation, loss of $C_3H_6$, oxidation | + | + | | + | |
| M11 | 5.40 | $C_{13}H_{12}O_4$ | 233.0808 | 233.0800 | −3.4 | 205.0500, 91.0562 | Loss of $C_2H_4$, mono-oxidation | | | | | + |
| M12 | 5.65 | $C_{20}H_{22}O_9$ | 407.1337 | 407.1337 | 0.0 | 231.0997, 175.0385, 91.0553 | Demethylation, glucuronide conjugation | | | + | + | |
| M13 | 5.78 | $C_{14}H_{12}O_3$ | 229.0859 | 229.0856 | −1.3 | 175.0389, 103.0550, 91.0562 | Demethylation, dehydrogenation | + | | | + | + |
| M14 | 5.79 | $C_{14}H_{14}O_4$ | 247.0965 | 247.0969 | 1.6 | 175.0395, 131.0494, 91.0565 | Demethylation, mono-oxidation | + | | | | + |
| M15 | 5.80 | $C_{14}H_{16}O_4$ | 249.1121 | 249.1123 | 0.8 | 231.1017, 177.0554, 147.0446, 91.0551 | Demethylation, hydrogenation, mono-oxidation | | | | | + |
| M16 | 6.34 | $C_{14}H_{14}O_4$ | 247.0965 | 247.0969 | 1.6 | 205.0556, 175.0390 | Demethylation, mono-oxidation | + | | + | | |
| M17 | 6.74 | $C_{13}H_{14}O_2$ | 203.1067 | 203.1065 | −1.0 | 161.0624, 131.0493, 91.0565 | Demethylation, loss of CO | | + | | + | |
| M18 | 6.90 | $C_{14}H_{14}O_4$ | 247.0965 | 247.0973 | 3.2 | 175.0397, 131.0493 | Demethylation, mono-oxidation | + | | | | |
| M19 | 6.95 | $C_{14}H_{16}O_4$ | 249.1121 | 249.1118 | −1.2 | 175.0390, 131.0498, 103.0553 | Demethylation, hydrogenation, mono-oxidation | | + | | | + |
| M20 | 7.41 | $C_{15}H_{14}O_6$ | 291.0863 | 291.0853 | −3.4 | 205.0564, 189.0562 | Dehydrogenation, tri-oxidation | | | | + | |
| M21 | 7.41 | $C_{15}H_{16}O_6$ | 293.1020 | 293.1022 | 0.7 | 205.0500, 131.0501, 91.0560 | Tri-oxidation | | | | + | + |
| M22 | 7.77 | $C_{14}H_{14}O_6S$ | 311.0584 | 311.0580 | −1.3 | 175.0397, 91.0554 | Demethylation, sulfate conjugation | | + | + | + | |
| M23 | 7.78 | $C_{14}H_{15}O_6P$ | 311.0679 | 311.0678 | −0.3 | 231.1021, 175.0396 | Demethylation, phosphorylation | | + | + | + | |
| M24 | 9.00 | $C_{14}H_{14}O_2$ | 215.1067 | 215.1055 | −3.7 | 173.0597, 131.0500 | Loss of $OCH_2$ | | | + | | |
| M25 | 9.06 | $C_{15}H_{12}O_5$ | 273.0758 | 273.0745 | −4.8 | 205.0505, 131.0499 | Dehydrogenation, di-oxidation | | | | + | + |
| M26 | 9.17 | $C_{15}H_{14}O_4$ | 259.0965 | 259.0977 | 4.6 | 243.1018, 189.0544 | Dehydrogenation, mono-oxidation | + | + | + | + | + |
| M27 | 9.19 | $C_{14}H_{14}O_5$ | 263.0914 | 263.0925 | 4.2 | 221.0447, 205.0493, 189.0548 | Demethylation, di-oxidation | | + | | | |
| M28 | 9.19 | $C_{14}H_{16}O_6$ | 281.1020 | 281.1018 | −0.7 | 189.0544, 177.0540, 147.0437 | Demethylation, mono-oxidation, oxydrolysis | | + | | | |
| M29 | 9.34 | $C_{15}H_{14}O_3$ | 243.1016 | 243.1019 | 1.2 | 213.0910, 201.0904, 189.0552, 159.0441 | Dehydrogenation | + | | | | |
| M30* | 9.54 | $C_9H_6O_3$ | 163.0390 | 163.0395 | 1.2 | 135.0441, 107.0490 | Demethylation, loss of $C_5H_8$ | + | | + | | |
| M31 | 9.68 | $C_{13}H_{12}O_3$ | 217.0859 | 217.0874 | 3.1 | 189.0544, 159.0437 | Loss of $C_2H_4$ | | | | + | + |
| M32 | 9.90 | $C_{14}H_{14}O_4$ | 247.0965 | 247.0969 | 2.3 | 191.0478, 163.0303, 107.0190 | Demethylation, mono-oxidation | + | | | | |
| M33 | 9.93 | $C_{15}H_{16}O_4$ | 261.1121 | 261.1118 | 1.6 | 243.1027, 189.0558, 131.0501, 103.0556 | Mono-oxidation | + | | | + | + |
| M34* | 10.11 | $C_{11}H_6O_3$ | 187.0390 | 187.0392 | −1.1 | 159.0442 | Demethylation, loss of $C_3H_6$, oxidation, loss of $H_2O$ | + | | | | + |

This journal is © The Royal Society of Chemistry 2018

Open Access Article. Published on 19 April 2018. Downloaded on 3/9/2025 2:44:59 PM.
This article is licensed under a Creative Commons Attribution-NonCommercial 3.0 Unported Licence.





Table 1 (*Contd.*)

| Compound ID | Retention time (min) | Formula | Calculated *m/z* [M + H] | Experimental *m/z* [M + H] | Error (ppm) | Product ions | Potential pathways | Source | | | | |
|---|---|---|---|---|---|---|---|---|---|---|---|---|
| | | | | | | | | RLMs | P | B | U | F |
| M35 | 10.12 | $C_{12}H_8O_3$ | 201.0546 | 201.0540 | 1.1 | 189.0550, 161.0620 | Dehydrogenation, loss of $C_3H_8$ | + | | | | + |
| M36 | 10.26 | $C_{15}H_{14}O_3$ | 243.1016 | 243.1010 | −3.0 | 213.0913, 201.0904, 189.0556, 159.0437, 131.0503 | Dehydrogenation | + | + | + | | + |
| M37 | 10.40 | $C_{15}H_{16}O_7S$ | 341.0690 | 341.0674 | −2.5 | 261.1153, 205.0497, 177.0654, 149.0606 | Mono-oxidation, sulfate conjugation | | + | + | + | |
| M38 | 10.41 | $C_{15}H_{16}O_5$ | 277.1071 | 277.1077 | −4.7 | 189.0544, 91.0556 | Di-oxidation | | + | + | + | |
| M39 | 10.65 | $C_{21}H_{24}O_{10}$ | 437.1442 | 437.1439 | 2.2 | 261.1123, 205.0499 | Mono-oxidation, glucuronide conjugation | | + | + | + | |
| M40 | 10.68 | $C_{15}H_{16}O_5$ | 277.1071 | 277.1073 | −0.7 | 205.0499, 91.0551 | Di-oxidation | + | | | | |
| M41 | 10.70 | $C_{15}H_{18}O_5$ | 279.1227 | 279.1219 | 0.7 | 245.1169, 223.0526, 149.0239, 119.0503 | Oxydrolysis | + | | | + | + |
| M42 | 10.80 | $C_{18}H_{21}NO_5S$ | 364.1213 | 364.1220 | −2.9 | 189.0562, 161.0605 | *S*-cysteine conjugation | | + | + | + | |
| M43 | 11.06 | $C_{10}H_6O_4$ | 191.0339 | 191.0334 | 1.9 | 107.0506, 91.0564 | Demethylation, mono-oxidation, loss of $C_4H_8$ | | | | | + |
| M44 | 11.07 | $C_{15}H_{14}O_5$ | 275.0914 | 275.0904 | −2.6 | 189.0549, 159.0441, 131.0496 | Dehydrogenation, di-oxidation | + | + | + | + | + |
| M45 | 11.13 | $C_{14}H_{14}O_4$ | 247.0965 | 247.0966 | −3.6 | 191.0476, 163.0305, 107.0193 | Demethylation, mono-oxidation | + | | | + | + |
| M46 | 11.29 | $C_{13}H_{14}O_3$ | 219.1016 | 219.1022 | 0.4 | 165.0541, 135.0440, 91.0562 | 3,4-Epoxide, demethylation, dehydrogenation, aldehylation | | | + | + | |
| M47 | 11.38 | $C_{21}H_{24}O_{10}$ | 437.1442 | 437.1448 | 2.7 | 261.1127, 205.0503 | Mono-oxidation, glucuronide conjugation | | + | + | + | |
| M48 | 11.51 | $C_{15}H_{18}O_5$ | 279.1227 | 279.1219 | 1.4 | 245.1169, 189.0555, 91.0560 | Oxydrolysis | + | | | | + |
| M49 | 11.81 | $C_{15}H_{16}O_4$ | 261.1121 | 261.1120 | −2.9 | 243.1025, 189.0556 | Mono-oxidation | + | | + | + | |
| M50 | 11.83 | $C_{15}H_{18}O_4$ | 263.1278 | 263.1265 | −0.4 | 245.1179, 189.0562 | Ester hydrolysis | + | | | | + |
| M51 | 11.83 | $C_{15}H_{14}O_3$ | 243.1016 | 243.1011 | −4.9 | 213.0910, 201.0900, 189.0555, 159.0433, 131.0501 | Dehydrogenation | + | | + | | |
| M52 | 11.93 | $C_{13}H_{12}O_7$ | 281.0656 | 281.0649 | −2.1 | 253.0707, 189.0563 | Qur-oxidation, loss of $C_2H_4$ | + | | + | | |
| M53 | 11.93 | $C_{13}H_{14}O_3$ | 219.1016 | 219.1012 | −2.5 | 165.0541, 135.0440, 91.0560 | 3,4-Epoxide, demethylation, dehydrogenation, aldehylation | | | + | + | |
| M54 | 12.12 | $C_{21}H_{24}O_{10}$ | 437.1442 | 437.1436 | −1.8 | 261.1119, 205.0497 | Mono-oxidation, glucuronide conjugation | | + | + | + | |
| M55 | 12.18 | $C_{14}H_{16}O_3$ | 233.1172 | 233.1171 | −1.4 | 149.0599, 91.0563 | 3,4-Epoxide, dehydrogenation, aldehylation | | | + | | + |
| M56 | 12.79 | $C_{15}H_{16}O_4$ | 261.1121 | 261.1130 | −0.4 | 205.0500, 175.0393, 91.0564 | Mono-oxidation | + | | | | |
| M57 | 12.94 | $C_{14}H_{14}O_3$ | 231.1016 | 231.1014 | 3.4 | 189.0550, 91.0555 | Demethylation | | | | | + |
| M58 | 13.04 | $C_{13}H_{12}O_7$ | 281.0656 | 281.0666 | −0.9 | 151.0317 | Qur-oxidation, loss of $C_2H_4$ | + | | + | | |
| M59 | 13.05 | $C_{15}H_{14}O_4$ | 259.0965 | 259.0958 | 3.6 | 243.1016, 205.0505, 189.0554, 131.0502 | Dehydrogenation, mono-oxidation | + | | + | | + |
| M60 | 13.60 | $C_{14}H_{14}O_3$ | 231.1016 | 231.1016 | −2.7 | 175.0396, 147.0445, 119.0497, 91.0558 | Demethylation | + | | | | + |
| M61 | 13.61 | $C_{10}H_6O_3$ | 175.0390 | 175.0385 | 0.0 | 160.0152, 147.0446 | Demethylation, loss of $C_4H_8$ | + | | | + | + |
| M62 | 14.39 | $C_{14}H_{16}O_4$ | 249.1121 | 249.1130 | −2.9 | 231.1040, 177.0539, 91.0536 | 3,4-Epoxide, dehydrogenation, aldehylation, oxidation | | | + | | |
| M63 | 14.50 | $C_{15}H_{16}O_4$ | 261.1121 | 261.1118 | 3.6 | 205.0504, 175.0390, 91.0565 | Mono-oxidation | + | | | + | + |
| M64 | 14.56 | $C_{14}H_{14}O_4$ | 247.0965 | 247.0965 | −1.1 | 191.0472, 163.0307 | Demethylation, mono-oxidation | + | | | | |
| M65 | 15.14 | $C_{14}H_{16}O_4$ | 249.1121 | 249.1118 | 0.0 | 193.0495, 165.0535 | Di-oxidation, loss of CO | | | + | | |
| M66* | 15.36 | $C_{10}H_8O_4$ | 193.0495 | 193.0491 | −1.2 | 165.0548 | Mono-oxidation, loss of $C_5H_8$ | | | + | + | |
| M67 | 16.28 | $C_{20}H_{23}NO_6S$ | 406.1319 | 406.1330 | −2.1 | 245.1173, 189.0544 | *N*-Acetylcysteine conjugation | | | + | + | + |
| M68 | 16.81 | $C_{15}H_{16}O_4$ | 261.1121 | 261.1130 | 2.7 | 205.0500, 175.0391, 91.0560 | Mono-oxidation | + | | | + | + |

This journal is © The Royal Society of Chemistry 2018

Open Access Article. Published on 19 April 2018. Downloaded on 3/9/2025 2:44:59 PM.
This article is licensed under a Creative Commons Attribution-NonCommercial 3.0 Unported Licence.

Table 1 (*Contd.*)

| Compound ID | Retention time (min) | Formula | Calculated *m/z* [M + H] | Experimental *m/z* [M + H] | Error (ppm) | Product ions | Potential pathways | Source | | | |
|---|---|---|---|---|---|---|---|---|---|---|---|
| | | | | | | | | RLMs | P | B | U | F |
| M69 | 17.77 | $C_{14}H_{16}O_2$ | 217.1223 | 217.1224 | 3.4 | 202.0985, 161.0604, 133.0656 | Loss of CO | | | + | | + |
| M70 | 17.80 | $C_{14}H_{18}O_3$ | 235.1329 | 235.1320 | 0.5 | 217.1223, 161.0788 | Loss of CO, hydrolysis | | | + | | + |
| M71 | 18.88 | $C_{15}H_{16}O_4$ | 261.1121 | 261.1122 | −3.8 | 205.0503, 175.0388, 91.0568 | Mono-oxidation | + | | + | + | + |
| M72 | 20.65 | $C_{15}H_{18}O_3$ | 247.1329 | 247.1326 | 0.4 | 191.0689, 161.0582, 133.0639, 103.0545, 77.0398 | Hydrogenation | + | | | | + |

[a] *: Confirmation in comparison with authentic standards; key product ions (KPIs) were underlined and indicated in bold face; RLMs: rat liver microsomes; P: plasma; B: bile; U: urine; F: feces; "+", detected.

by a loss of $H_2O_2$. So, M41 and M48 were tentatively identified as oxydrolysis metabolites of M0. According to our knowledge, the possible metabolism sites were C3-C4 and C-2′-C-3′.[28] The significant product ion at *m/z* 223.0526 of M41 was 34 Da higher than *m/z* 189.0554 of OST, which indicated that oxydrolysis occured at C-2′-C-3′. Therefore, M41 was identified as C-2′-C-3′ oxydrolysis metabolites of M0, and M48 was identified as C-3-C-4 oxydrolysis metabolites of M0.[28]

**3.2.7. Hydrogenation metabolites.** M72 was eluted at 20.65 min possessing the protonated molecular ion $[M + H]^+$ at *m/z* 247.1326, 2 Da (2H) higher than that of OST, suggesting that it underwent hydrogenation reaction. The product ions at *m/z* 191.0689, *m/z* 161.0582 and *m/z* 133.0639 were also 2 Da higher than that of M0, indicating hydrogenation occurred at the basic rings. The other product ions at *m/z* 103.0545 and *m/z* 77.0398 implied that the exact site of hydrogenation was C-3-C-4 of OST.[28]

**3.2.8. Metabolites *via* losing $CH_2O$, $C_2H_4$, $C_3H_8$, $C_5H_8$ or CO.** M24 ($t_R$ = 9.00 min) gave an $[M + H]^+$ ion at *m/z* 215.1059 ($C_{14}H_{14}O_2$), which was 30 Da ($CH_2O$) lower than OST. The $[M + H]^+$ showed the product ions at $[M + H–C_3H_6]^+$ *m/z* 173.0597 and $[M + H–CO–C_4H_8]^+$ *m/z* 131.0500, which were similar to that of M0. Therefore, M24 was tentatively identified as losing a group of $CH_2O$ at C-7 from OST.

M31 was detected at 9.68 min and showed the molecular formula of $C_{13}H_{12}O_3$ ($[M + H]^+$ *m/z* 217.0864), which was 28 Da ($C_2H_4$) lower than that of M0. The characteristic product ions at *m/z* 189.0544 $[M + H–C_2H_4]^+$ and *m/z* 159.0437 $[M + H–C_2H_4–CH_2O]^+$ indicated that M31 might be the cleavage of side-chain alkyl $C_2H_4$.[28]

M69 was eluted at 17.77 min and exhibited the molecular formula of $C_{14}H_{16}O_2$ ($[M + H]^+$ *m/z* 217.1224), which was 28 Da (CO) lower than that of OST. The key product ions were at *m/z* 202.0985 $[M + H–CH_3]$, *m/z* 161.0604 $[M + H–C_4H_8]^+$ and *m/z* 133.0656 $[M + H–C_4H_8–CO]^+$. According to its cleavage rule of OST, decarbonylation might occur at C-2 from M0.

M35 ($t_R$ = 10.12 min) gave an $[M + H]^+$ at *m/z* 201.0540 with the molecular formula of $C_{12}H_8O_3$, which was 44 Da ($C_3H_8$) lower than that of OST. In the MS/MS spectrum, product ions at *m/z* 189.0550 and *m/z* 161.0620 were observed. Therefore, we deduced that M35 was loss of a group of $C_3H_8$ from side chain of parent drug.[28]

**3.2.9. Oxidation and dehydrogenation metabolites.** M2 ($t_R$ = 2.80 min), M4 ($t_R$ = 3.60 min), M7 ($t_R$ = 4.84 min), M26 ($t_R$ = 9.17 min) and M59 ($t_R$ = 13.05 min), exhibited the same molecular formula of $C_{15}H_{14}O_4$ ($[M + H]^+$ *m/z* 259.0965), 14 Da (O–2H) higher than that of OST. They were determined as the mono-oxidated product of dehydrogenated osthole. In their MS/MS spectra, they all showed the product ion $[M + H–O]^+$ at *m/z* 243.1014, which was the characteristic ion of dehydrogenated metabolites. However, M59 showed different product ions compared with M2, M4, M7 and M26, indicated that they were oxidized at different sites of the structure. Product ion at *m/z* 205.0505 of M59 implied that the mono-oxidation was conducted at C-3, C-4, C-5 or C-6 of OST. The other four metabolites were mono-oxidized at different site at side chain after compared with their values of Clog *P*.

Open Access Article. Published on 19 April 2018. Downloaded on 3/9/2025 2:44:59 PM.
This article is licensed under a Creative Commons Attribution-NonCommercial 3.0 Unported Licence.

**3.2.10. Demethylation and dehydrogenation metabolites.** M9 ($C_{14}H_{12}O_3$, *m*/*z* 229.0856, 5.21 min) and M13 ($C_{14}H_{12}O_3$, *m*/*z* 229.0856, 5.78 min) were a pair of isomers, which was 14 Da ($CH_2$) lower than that of M29, M36 or M51. In the MS/MS spectra, they both generated product ion at *m*/*z* 175.0387 $[M + H–C_4H_6]^+$. Accordingly, we could deduce that demethylation reaction occurred at the C-7's methoxy group.[16]

**3.2.11. Demethylation and oxidation metabolites.** M8 ($t_R$ = 5.18 min), M14 ($t_R$ = 5.79 min), M16 ($t_R$ = 6.34 min), M18 ($t_R$ = 6.90 min), M32 ($t_R$ = 9.90 min), M45 ($t_R$ = 11.13 min) and M64 ($t_R$ = 14.56 min), exhibited the same molecular formula of $C_{14}H_{14}O_4$ ($[M + H]^+$ *m*/*z* 247.0965), 2 Da ($O–CH_2$) higher than that of OST. They were determined as the mono-oxidized product of demethylated osthole. However, M16 showed the different product ions at *m*/*z* 205.0556 compared with the other six metabolites, indicated that it was oxidized at C-3, C-4, C-5 or C-6, and demethylation reaction was performed on the side chain of OST.

M32, M45 and M64 all showed diagnostic product ions at *m*/*z* 191.0478 and *m*/*z* 163.0303, which suggested that demethylation reaction might generate at C-7's methoxy group. M32 and M45 were both detected product ion at *m*/*z* 107.0190, which revealed that mono-oxidized could occur at C-5 or C-6 compared with that of parent drug. According to their values of Clog *P*, M32 was identified C-5 oxidized metabolites and M45 was identified C-6 oxidized metabolites of M60. M64 was temporarily confirmed as C-3 or C-4 oxidized metabolite of M60.[28]

M8, M14 and M18 was only detected the typical product ion at *m*/*z* 175.0393, which indicated that demethylation reaction might occur at C-7's methoxy group and mono-oxidation reaction might occur at side chain.[16]

**3.2.12. 3,4-Epoxide and aldehylation metabolites.** M46 and M53 were isomers with the similar fragment patterns. The protonated ion M46 was deduced as $C_{13}H_{14}O_3$ ($[M + H]^+$ *m*/*z* 219.1022). In the MS/MS spectrum, the $[M + H]^+$ ion gave similar fragment pathway with parent drug, who generated product ions at *m*/*z* 165.0541 $[M + H–C_4H_6]^+$ and *m*/*z* 135.0440 $[M + H–C_4H_6–CH_2O]^+$. According to our knowledge, it was identified as losing a group of methyl and carbon dioxide, suggesting further aldehylation happened on coumarin structure after formation of 3,4-epoxide.[16] Previous studies have proved that coumarin could be metabolized through cleavage of the lactone ring *via* 3,4-epoxide intermediate. However, coumarin 3,4-epoxide was not stable, and it degrades rapidly in aqueous conditions to form aldehyde metabolites with loss of carbon dioxide.[29,30]

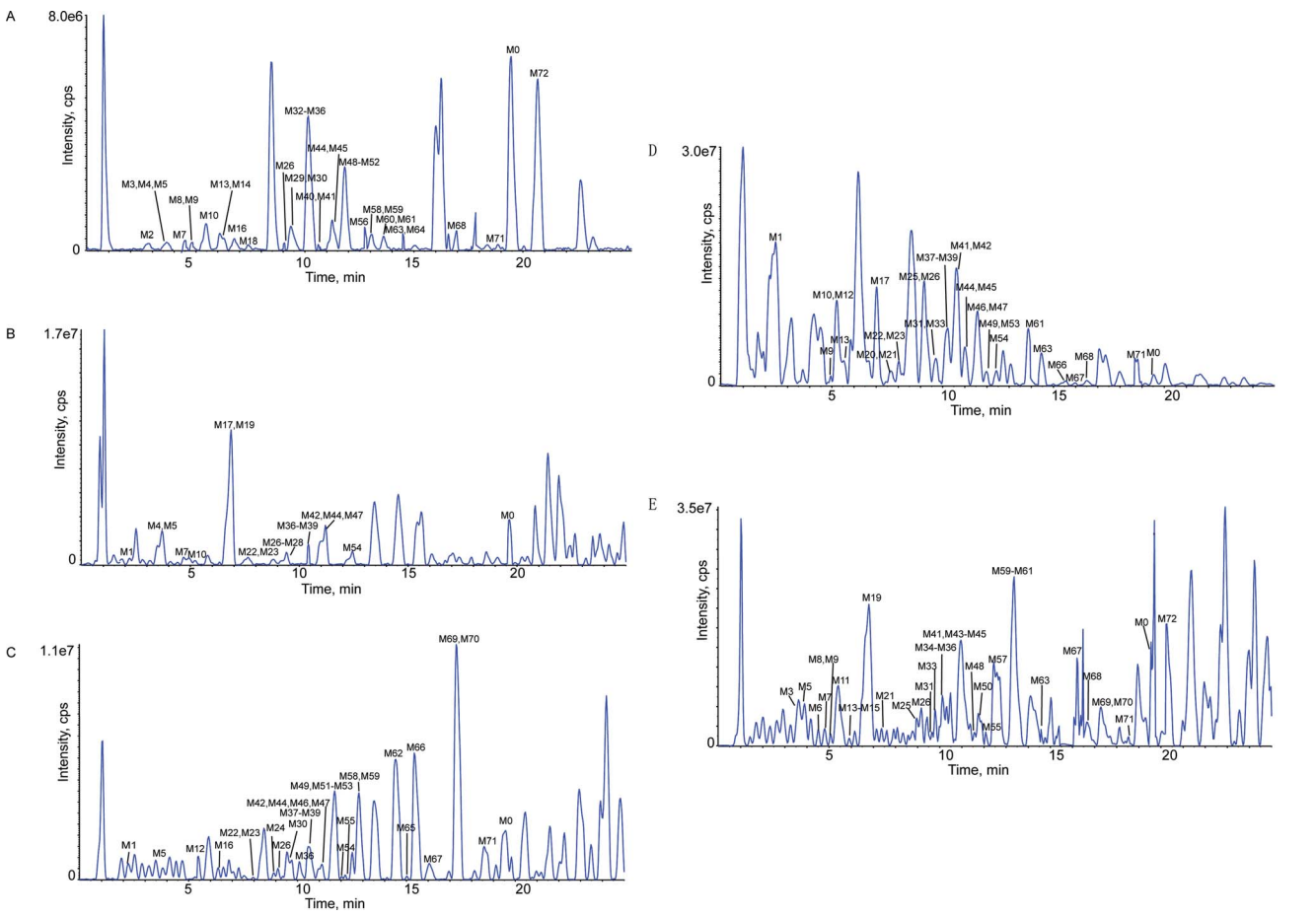


Fig. 2 TIC for the sample group in RLMs, rat plasma, rat bile, rat urine, rat feces. Panel A: TIC for the sample group in RLMs; Panel B: TIC for the sample group in rat plasma; Panel C: TIC for the sample group in rat bile; Panel D: TIC for the sample group in rat urine; Panel E: TIC for the sample group in rat feces.


This journal is © The Royal Society of Chemistry 2018

Open Access Article. Published on 19 April 2018. Downloaded on 3/9/2025 2:44:59 PM.
This article is licensed under a Creative Commons Attribution-NonCommercial 3.0 Unported Licence.

### 3.3. Phase II metabolites identification

A total of 10 phase II metabolites were identified in rats, and metabolic pathways involved sulfate conjugation, glucuronide conjugation, phosphorylation, *S*-cysteine conjugation and *N*-acetylcysteine conjugation. Deductions of representative phase II metabolite structures were summarized as follows. The retention times and product ions of the other metabolites were listed in Table 1.

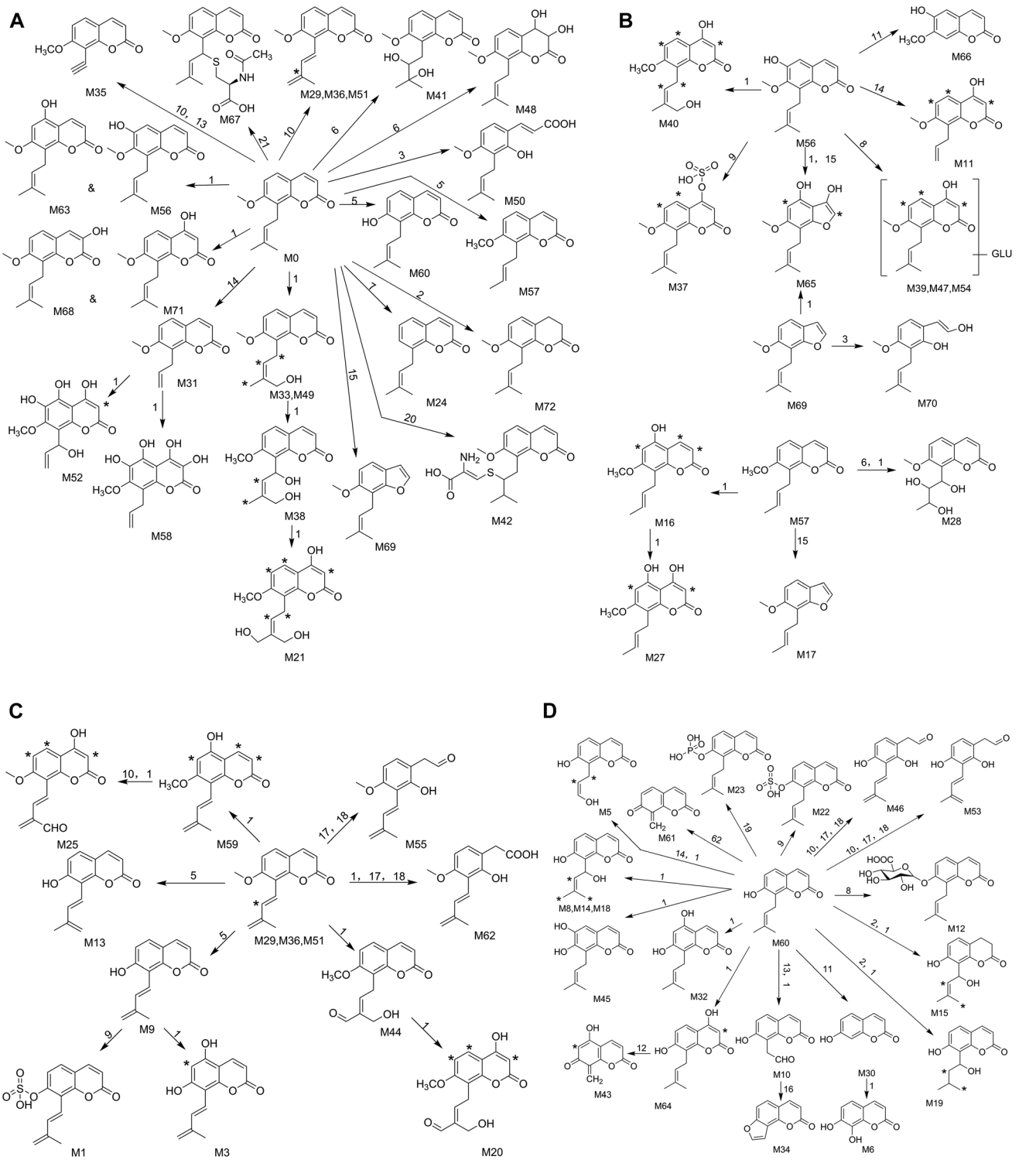


Fig. 3 The proposed osthole (M0) metabolic pathways *in vitro* and *in vivo* (1. oxidation, 2. hydrogenation, 3. hydrolysis, 4. methylation, 5. demethylation, 6. oxydrolysis, 7. loss of $OCH_2$, 8. glucuronide conjugation, 9. sulfate conjugation, 10. dehydrogenation, 11. loss of $C_5H_8$, 12. loss of $C_4H_8$, 13. loss of $C_3H_6$, 14. loss of $C_2H_4$, 15. loss of CO, 16. loss of $H_2O$, 17. 3,4-epoxide, 18. aldehylation, 19. phosphorylation, 20. *S*-cysteine conjugation, 21. *N*-acetylcysteine conjugation).

Open Access Article. Published on 19 April 2018. Downloaded on 3/9/2025 2:44:59 PM.
This article is licensed under a Creative Commons Attribution-NonCommercial 3.0 Unported Licence.

**3.3.1. Sulfate metabolites.** M1 was eluted at 2.19 min with the molecular formula of $C_{14}H_{12}O_6S$ ($[M + H]^+$ *m/z* 309.0422), which was 80 Da ($SO_3$) higher than that of M9 and M13. In its MS/MS spectrum, the $[M + H]^+$ ion showed product ions at *m/z* 229.0860 $[M + H–SO_3]^+$ and *m/z* 175.0398 $[M + H–SO_3–C_4H_6]^+$. Accordingly, M1 was determined as sulfate conjugate of M9 or M13.[28]

**3.3.2. Glucuronide conjugation metabolites.** M39 ($t_R$ = 10.65 min), M47 ($t_R$ = 11.38 min), and M54 ($t_R$ = 12.12 min) showed the same molecular formula of $C_{21}H_{24}O_{10}$. In their MS/MS spectra, the diagnostic product ions at *m/z* 261.1123 and *m/z* 205.0499 were generated by successive loss of one glucuronic acid and side-chain group ($C_4H_8$) from the $[M + H]^+$. So, the most likely structures of them were glucuronide conjugates of M56, M63, M68 or M71.[25] However, the exact binding sites were not confirmed in this study.

**3.3.3. Phosphorylate metabolite.** M23 was eluted at 7.78 min with the molecular formula of $C_{14}H_{15}O_6P$ ($[M + H]^+$ *m/z* 311.0678), which was 80 Da ($HPO_3$) higher than that of M57 and M60. In its MS/MS spectrum, the major product ions at *m/z* 231.1021 $[M + H–HPO_3]^+$ and *m/z* 175.0396 $[M + H–HPO_3–C_4H_8]^+$ suggested that M23 was inferred as phosphorylate conjugates of M60, which was observed in rat plasma, bile and urine after oral administration of OST for the first time.

**3.3.4. *S*-Cysteine metabolite.** M42 was detected at 10.80 min with the quasi-molecular ion at *m/z* 364.1220 ($C_{18}H_{21}NO_5S$), 119 Da ($C_3H_5NO_2S$) more than that of OST. In the MS/MS spectrum, the distinctive product ions at *m/z* 189.0562 and *m/z* 161.0605 were observed, which were obtained by the elimination of $C_3H_5NO_2S + C_4H_8$ and $C_3H_5NO_2S + C_4H_8 + CO$, respectively. In consideration of the activity of double bonds, we determined that *S*-cysteine conjugation reaction took place in side-chain double bond of M0.[28]

**3.3.5. *N*-Acetylcysteine metabolite.** M67 was observed at 16.28 min and possessed the predominant quasi-molecular ion $[M + H]^+$ at *m/z* 406.1330 ($C_{20}H_{23}NO_6S$), 161 Da heavier than that of OST, suggesting that it was a $C_5H_7NO_3S$ conjugation product of M0. In the MS/MS spectrum, the characteristic product ions at *m/z* 245.1173 and *m/z* 189.0544 were formed by the loss of $C_5H_7NO_3S$ and $C_5H_7NO_3S + C_4H_8$, respectively. According to the activity of hydrogen atoms, *N*-acetylcysteine conjugation reaction was determined at the site of C-1′, which was never observed in rat sample after oral administration of OST.[28]

### 3.4. Metabolic profiles of OST

This study was conducted to elucidate the metabolism of OST *in vitro* (RLMs) and *in vivo* (plasma, bile, urine, feces of rats). The involved biotransformation and mass changes were listed in the Table S1.† TIC for the sample group in RLMs, rat plasma, bile, urine and feces were exhibited at Fig. 2. Based on the identified metabolites (Table 1), the proposed metabolic pathways for OST were shown in Fig. 3, and the representative MS/MS spectra and proposed fragmentation pathways of M12, M33, M37, M41, M46, M56, M60 and M62 were showed in Fig. S2.† The main metabolic pathways for OST were mono-oxidation, demethylation, dehydrogenation, oxydrolysis, 3,4-epoxide, aldehylation. The predominant phase II metabolite reaction mainly underwent sulfate conjugation, glucuronide conjugation, phosphorylation, *S*-cysteine conjugation and *N*-acetylcysteine conjugation.

Thirty-nine metabolites were identified in RLMs, indicated that most metabolites could be excreted in RLMs samples and RLMs samples are suitable for rapid identification of metabolites of OST *in vitro*. It also verified that liver is considered as the most important organ in the biotransformation of drugs with a variety of required enzymes especially for cytochrome P450 (CYP) enzymes. They are the major drug metabolizing enzymes that play an important role in xenobiotic metabolism.[31] Rat bile, urine and feces also possessed high activity for OST metabolism, which were observed 32, 32 and 37 metabolites, respectively. Only twenty metabolites were detected in rat plasma, implied that rat plasma might hold low biotransformation activity in plasma.

Among all the metabolites, M6, M30, M34 and M66 were confirmed by comparing with standard substances in terms of the retention times and MS/MS product ions. Comparing with the metabolism in different bio-samples, it was found that oxidation, dehydrogenation, demethylation and oxydrolysis were major biotransformations *in vitro*, and loss of side-chain alkyl, 3,4-epoxide, aldehylation, hydrogenation, loss of CO, a series of conjugation reactions *in vivo*. More significantly, the metabolites which underwent loss of side-chain alkyl, loss of CO, loss of $OCH_2$, oxydrolysis, *S*-cysteine conjugation, sulfate conjugation, phosphorylation and *N*-acetylcysteine conjugation reactions were tentatively identified in rats or RLMs for the first time. M6 (daphnetin), M30 (7-hydroxycoumarin), M34 (isopsoralen) and M66 (isoscopoletin) have been proved that hold immunosuppressive,[32] antinociceptive, anti-inflammatory,[33] antitumor[34] and inhibitory[35] properties, respectively. These results provide some insights into understanding the metabolic profiles of OST, which could guide the pharmacokinetics investigation of OST and its major metabolites in the clinic.

## 4. Conclusions

In conclusion, a rapid and practical analytical method based on UHPLC-Q-TOF-MS was developed for the characterization of OST metabolites *in vitro* and *in vivo*. A novel SWATH acquisition method was used for detected most metabolites of OST with a high hit rate and quality by means of PCVG filtering function for the first time. A total of 62 phase I metabolites and 10 phase II metabolites of OST were identified *in vitro* and *in vivo*, including 39 metabolites in RLMs, 20 metabolites in rat plasma, 32 metabolites in rat bile, 32 metabolites in rat urine and 37 metabolites in rat feces samples. The characteristic metabolic bio-transformation routes of phase I were oxydrolysis, demethylation, 3,4-epoxide, and aldehylation. Glucuronide conjugation, *S*-cysteine conjugation, sulfate conjugation, phosphorylation and *N*-acetylcysteine conjugation reactions were main metabolic pathways of phase II. This proposed biotransformation routes of OST provide scientific and reliable support for full understanding of the metabolism of coumarins. Furthermore, the novel strategy was a powerful tool for

 This journal is © The Royal Society of Chemistry 2018

Open Access Article. Published on 19 April 2018. Downloaded on 3/9/2025 2:44:59 PM.
This article is licensed under a Creative Commons Attribution-NonCommercial 3.0 Unported Licence.

constituents and metabolites identification, and preparation of the active metabolites will be greatly helpful in elucidating the potential biological mechanism of coumarin derivatives in clinical application.

## Conflicts of interest

The authors declare that they have no conflict of interest.

## Acknowledgements

The work received financial support from the National Natural Science Foundation of China (no. 81473180). All of the authors are grateful for the support from Department of Pharmaceutical Analysis of school of Pharmacy in Hebei Medical University.

## References

1 Chinese Pharmacopoeia Commission, *The Pharmacopoeia of the People's Republic of China, Part I*, China Medical Science Press, Beijing, China, 2015, p. 315.
2 S. Vogl, M. Zehl, P. Picker, E. Urban, C. Wawrosch, G. Reznicek, J. Saukel and B. Kopp, *J. Agric. Food Chem.*, 2011, **59**, 4371–4377.
3 E. P. Siskos, B. E. Mazomenos and M. A. Konstantopoulou, *J. Agric. Food Chem.*, 2008, **56**, 5577–5581.
4 I. Jerković, J. Drulžić, Z. Marijanović, M. Gugić, S. Jokić and M. Roje, *Nat. Prod. Commun.*, 2015, **10**, 1315–1318.
5 L. Liu, J. Mao, Q. Wang, Z. Zhang, G. Wu, Q. Tang, B. Zhao, L. Li and Q. Li, *Biomed. Pharmacother.*, 2017, **94**, 1020–1027.
6 Y. Li, Y. Li, F. Shi, L. Wang, L. Li and D. Yang, *Eur. J. Pharmacol.*, 2017, **818**, 525–533.
7 X. Zhu, X. Song, K. Xie, X. Zhang, W. He and F. Liu, *Int. J. Mol. Med.*, 2017, **40**, 1143–1151.
8 Y. Shokoohinia, S. Khajouei, F. Ahmadi, N. Ghiasvand and L. Hosseinzadeh, *Iran. J. Basic Med. Sci.*, 2017, **20**, 438–445.
9 Y. Yan, L. Kong, Y. Xia, W. Liang, L. Wang, J. Song, Y. Yao, Y. Lin and J. Yang, *Brain, Behav., Immun.*, 2018, **67**, 118–129.
10 P. P. Song, J. Zhao, Z. L. Liu, Y. B. Duan, Y. P. Hou, C. Q. Zhao, M. Wu, M. Wei, N. H. Wang, Y. Lv and Z. J. Han, *Pest Manage. Sci.*, 2017, **73**, 94–101.
11 Z. Wang, J. R. Kim, M. Wang, S. Shu and Y. J. Ahn, *Pest Manage. Sci.*, 2012, **68**, 1041–1047.
12 X. Zhang, Y. Yao, Y. Lou, H. D. Jiang, X. W. Wang, X. J. Chai and S. Zeng, *Drug Metab. Dispos.*, 2010, **38**, 2157–2165.
13 T. H. Tsai, T. R. Tsai, C. C. Chen and F. C. Chen, *J. Pharm. Biomed. Anal.*, 1996, **14**, 749–753.
14 M. Liu, H. Liu, X. Lu, C. Li, Z. Xiong and F. Li, *J. Chromatogr. B: Anal. Technol. Biomed. Life Sci.*, 2007, **860**, 113–120.
15 F. Yun, A. Kang, J. Shan, X. Zhao, X. Bi and L. Di, *Biomed. Chromatogr.*, 2013, **27**, 676–680.
16 J. Li and W. Chan, *J. Pharm. Biomed. Anal.*, 2013, **74**, 156–161.
17 Q. Zhao, X. M. Li, H. N. Liu, F. J. Gonzalez and F. Li, *Xenobiotica*, 2018, **48**, 285–299.
18 X. Lv, C. Y. Wang, J. Hou, B. J. Zhang, S. Deng, Y. Tian, S. S. Huang, H. L. Zhang, X. H. Shu, Y. H. Zhen, K. X. Liu, J. H. Yao and X. C. Ma, *Xenobiotica*, 2012, **42**, 1120–1127.
19 Z. T. Yuan, H. Y. Xu, K. Wang, Z. H. Zhao and H. Ming, *J. Pharm. Biomed. Anal.*, 2009, **49**, 1226–1232.
20 Y. J. Yoon, K. B. Kim and H. Kim, *Drug Metab. Dispos.*, 2007, **35**, 1518–1524.
21 L. F. Zhang, X. Hu, P. Wang and L. Zhang, *Acta Pharm. Sin. B*, 2009, **44**, 1131–1135.
22 H. Xiao, H. Wei and Y. Yuan, *Eur. J. Drug Metab. Pharmacokinet.*, 2015, **40**, 373–377.
23 I. Chernushevich, A. V. Loboda and B. A. Thomson, *J. Mass Spectrom.*, 2001, **36**, 849–865.
24 K. B. Scheidweiler, M. J. Jarvis and M. A. Huestis, *Anal. Bioanal. Chem.*, 2015, **407**, 883–897.
25 W. Xie, Y. Jin, L. Hou, Y. Ma, H. Xu, K. Zhang, L. Zhang and Y. Du, *J. Pharm. Biomed. Anal.*, 2017, **145**, 865–878.
26 L. Semenec, A. E. Laloo, B. L. Schulz, I. A. Vergara, P. L. Bond and A. E. Franks, *Bioelectrochemistry*, 2018, **119**, 150–160.
27 X. Zhang, J. T. Yin, C. J. Liang, Y. P. Sun and L. T. Zhang, *J. Agric. Food Chem.*, 2017, **65**, 10959–10972.
28 G. Song, M. Jin, Y. Du, L. Cao and H. Xu, *J. Chromatogr. B: Anal. Technol. Biomed. Life Sci.*, 2016, **1022**, 21–29.
29 S. L. Born, A. M. Api, R. A. Ford, F. R. Lefever and D. R. Hawkins, *Food Chem. Toxicol.*, 2003, **41**, 247–258.
30 D. F. Lewis, Y. Ito and B. G. Lake, *Toxicol. In Vitro*, 2006, **20**, 256–264.
31 F. P. Guengerich, *Chem. Res. Toxicol.*, 2008, **21**, 70–83.
32 B. Song, Z. Wang, Y. Liu, S. Xu, G. Huang, Y. Xiong, S. Zhang, L. Xu, X. Deng and S. Guan, *PLoS One*, 2014, **9**, e96502.
33 T. A. Barros, L. A. de Freitas, J. M. Filho, X. P. Nunes, A. M. Giulietti, G. E. de Souza, R. R. dos Santos, M. B. Soares and C. F. Villarreal, *J. Pharm. Pharmacol.*, 2010, **62**, 205–213.
34 Y. Wang, C. Hong, C. Zhou, D. Xu and H. B. Qu, *J. Evidence-Based Complementary Altern. Med.*, 2011, **2011**, 363052.
35 M. Y. Ali, S. Jannat, H. A. Jung, R. J. Choi, A. Roy and J. S. Choi, *Asian Pac. J. Trop. Med.*, 2016, **9**, 103–111.